https://doi.org/10.1016/j.measurement.2016.12.005 This is the Pre-Published Version.

Validation of a 3D foot scanning system for evaluation of forefoot shape with elevated heels

Frances KW Wan, Kit-Lun Yick*, Winnie WM Yu

Institute of Textiles and Clothing, The Hong Kong Polytechnic University, Hunghom, Hong Kong

Abstract

The toe box design is a crucial element for footwear comfort in high-heeled shoes. Their shoe lasts, however, are developed based on foot measurements taken under a foot-flat condition. There lacks investigations on whether the forefoot shape changes with elevated heels.

In this study, we have developed a rapid 3D foot scanning system to acquire 3D foot anthropometric measurements of elevated heels. The system's repeatability and accuracy are validated. Foot scanning is then performed on 45 female subjects in three conditions: foot-flat (0cm), elevated mid-heel (5cm) and high-heel (10cm). Eighteen forefoot measurements are extracted to evaluate the changes in the forefoot shape.

Our newly developed system is proven to be highly repeatable (±0.5mm) and adequately accurate (±0.8mm) to carry out foot anthropometric measurements. We find that with increases in heel height, the fourth and fifth metatarsal-phalangeal joints will be raised and the small toe will migrate towards the lateral side.

Key words: 3D foot scanning, Foot anthropometry, High-heeled shoes, Toe box

1. Introduction

Having long become part of the female attire in the western cultures, high-heeled shoes (HHSs) were worn by a large population of women around the world every day. However, HHSs have been found to be the most common culprit of foot pain when compared with other types of shoes. In a survey conducted by the American Podiatric Medical Association in 2014, 71% of HHS owners reported foot pain when wearing HHSs. However, 39% continued to wear HHSs on a weekly basis [1].

Over the past decades, many researchers have reported the adverse effects of wearing HHSs. Elevated heels change the morphology and weight bearing conditions of the feet, thus greatly increasing the forefoot plantar pressure [2-5], and resulting in pain in the forefoot.

In addition to foot pain and discomfort, ill-fitting HHSs could also further damage foot health. Improper shoe box designs could increase mutual compression of the toes and pressure between the toes and shoe sole [6]. Ill-fitting HHSs might cause the foot to slide down the footbed, thus causing

pain, discomfort, corns, bunions and toe deformation in the long run [7]. However, out of aesthetic considerations, the design of HHSs always comes with a narrow base and a pointed toe box. As a result, most HHSs are actually too narrow to be worn.

In fact, studies have shown that women tend to wear shoes that are more narrow than their actual foot width [8,9], and a high degree of correlation was found between ill-fitting footwear and foot pain [10]. As the human foot is an important organ for weight bearing and locomotion, health problems may arise from improper footwear. Walking in ill-fitting footwear can therefore lead to foot deformities in the long run.

Ensuring the proper fit of HHSs, therefore, would be greatly beneficial to foot health. To achieve the proper shoe fit, the 3-dimensional (3D) shoe shape should match well with the foot shape of the wearer [11,12]. To evaluate the match between the shape of a foot and the shoe sole, researchers usually compare the foot dimensions with the shoe last of the shoe of interest. With the evolution of 3D scanning technologies, many studies have been conducted to evaluate shoe fit by comparing the shape of the shoe last and human feet [13-16]. These studies, however, have focused on ordinary low-heeled shoes. Kouchi and Tsutsumi [17] evaluated the 3D foot shape of 39 female subjects who stood on foot platforms to simulate heel heights of 0 cm, 4 cm and 8 cm by using 3D scanning technology, but no evaluation was carried out on the forefoot region.

Since forefoot loading is significantly increased as the heel height increases, HHS wearers might naturally adopt new strategies in their foot postures, such as placement adjustment of their toes to maintain balance control and provide better support for their entire body. Foot measurements and shape characteristics of the forefoot region, have therefore, become more important in HHSs.

The importance of the fit of the forefoot regions of ladies shoes, indeed, has been recognised in recent studies. Au and Goonetilleke [18] evaluated the fit preferences in different regions of ladies shoes. Significant fit preferences were found in four of the seven regions, where two of them, namely, the toe and the metatarsophalangeal regions, are part of the forefoot region. Branthwaite et al. [6] suggested that the high prevalence of pain and discomfort experienced by HHS wearers is generally associated with the toe box design and the shoe volume. These results indicate that the shoe fit of the forefoot area is crucial for the overall foot comfort perceived by the wearer.

Anthropometric measurements of the forefoot region could help shoe manufacturers to improve HHS designs for better comfort and foot health. For example, the ball width, and toe heights and angles can help to design the toe box dimensions, whereas the location of the metatarsophalangeal joints can help to determine the stiffness or flexibility of different parts of the shoes [19].

In order to determine whether the shape characteristics of the forefoot regions vary with heel elevation, a systematic study is required to collect 3D foot measurements in different heel height conditions. An analysis can then be carried out to evaluate the shape characteristics of the forefoot region by examining the linear dimensions and toe angles.

Therefore, the primary aims of the present study are:

(1) to describe the development and evaluation of a rapid 3D foot scanning system for acquiring 3D foot anthropometric measurements of elevated heels,
(2) to collect 3D foot measurements of female subjects who are standing on foot platforms that simulate different heel height conditions, which range from flat horizontal (0 cm), elevated mid-heel (5 cm) to high-heel (10 cm) with the use of 3D scanning technology, and
(3) to investigate how the shape characteristics of the forefoot change with different heel heights. The shape characteristics of the forefoot are described by using 18 measurement parameters.

2. Methodology

2.1 Development of 3D Foot and Ankle Scanning System

Although 3D foot scanning has been extensively utilised in the footwear industry, specific information on foot anthropometric measurements of elevated heels is particularly scarce. The lack of 3D scanning equipment might be one of the reasons for this deficiency of information. Foot scanners available in the market only allow the foot to be scanned in a designated foot flat position. Problems would arise when scanning a heel-elevated foot [20]. In this study, a 3D foot and ankle scanning system (Figure 1) is developed which enables a 360° scan with full colour texture and can be performed within a timeframe of one second.

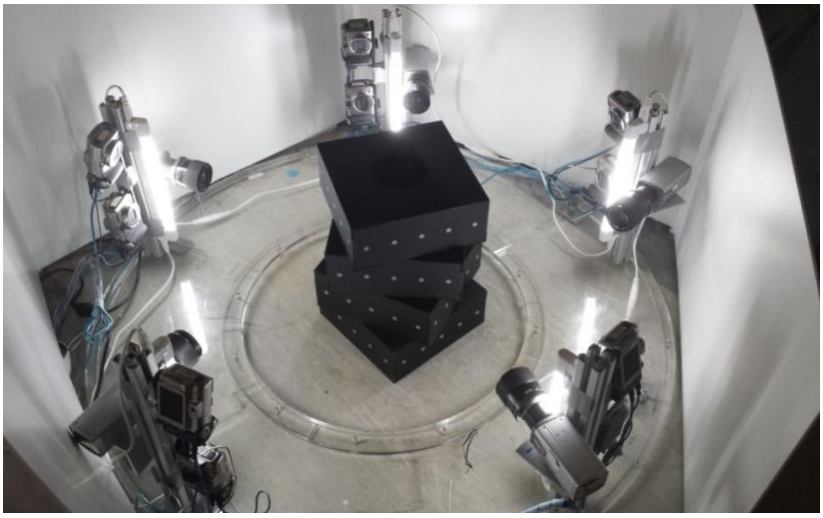

Figure 1 – Newly developed 3D foot and ankle scanning system

2.1.1 System Infrastructure

The 3D foot scanning system comprises five scanning modules. Each module includes a pair of Canon Powershot A650IS digital cameras (1.2 M pixels), a pattern projector and a 12-inch fluorescent tube. The camera settings, such as shutter speed, zoom factor and aperture size, were individually configured and locally stored in the cameras. These settings were automatically resumed when the cameras are switched on. All of the cameras were connected to two control units, through which the power supply and command signals were sent to the cameras. The two control units were each connected to their own laptop computer with a USB cable, and the laptops were connected to each other with a LAN cable.

The system of digital cameras, pattern projectors, control units, and the operation programme were previously developed by the Industrial Centre of The Hong Kong Polytechnic University as a portrait scanning system. In the present study, modifications are made to the instruments on the size of the projected pattern, number of scanning modules to be adopted, and their location and orientation. These parameters were carefully examined so that the best scanning coverage and level of details can be attained in the final foot model.

2.1.2 Camera Calibration

All of the cameras had to be calibrated prior to scanning. Their extrinsic orientation parameters, which include the camera positions (Cx, Cy, Cz) and rotation angles (phi, omega, kappa) in the Cartesian coordinate system, together with the intrinsic parameters that provide focal lengths (fx, fy), image centres (x0, y0), coefficients of radial lens distortions (k1, k2) and tangential distortions (p1, p2) were determined during the calibration process. The computation algorithm was written based on the work of Heikkilä & Silvén [21]. A 4-layer calibration range (Figure 2) was designed and fabricated for the calibration procedure. The 4-layers consisted of acrylic that is 0.5 cm in thickness with a black mat surface. Each layer has four sides. Five retro-reflective circular targets were attached onto each side. A total of 80 circular targets were attached across the whole calibration range. The positions of these targets were carefully surveyed by using close-range photogrammetry.

Figure 2 – The calibration range

Calibration accuracy is affected if the observed targets lie on the same plane. The four layers were therefore rotated at 45 degrees as they stacked up. By doing so, the targets captured by every camera would lie on various planes, which ensured system accuracy across a larger depth of field after calibration. Under such a target array arrangement, at least 25 targets would be captured by each camera during calibration, thus providing redundancy to resolve the calibration parameters.

2.1.3 3D scanning procedures

Two consecutive images were taken by each camera within 1 second during the scanning process. The first image recorded the real colour and texture information of the scanned foot while the second image was used to compute the anthropometric measurements of the foot. Computation algorithms were used to automatically process the images and rebuild the 3D models. For each image pair, point features that can be identified in both images were extracted. Lens distortion corrections were then made to the image coordinates of these point features in accordance with the intrinsic parameters obtained from the camera calibration. The 3D coordinates of each identical feature point were then computed based on photogrammetry. The raw data output of the 3D foot and ankle scanning system consisted of five aligned colour point clouds (Figure 3) reconstructed from the image pair of each scanning module. Further post-processing could be carried out by using any 3D modeling software to produce mesh models. High definition colour textural information was finally mapped onto the 3D model with the texture mapping algorithms of the system based on the camera calibration parameters.

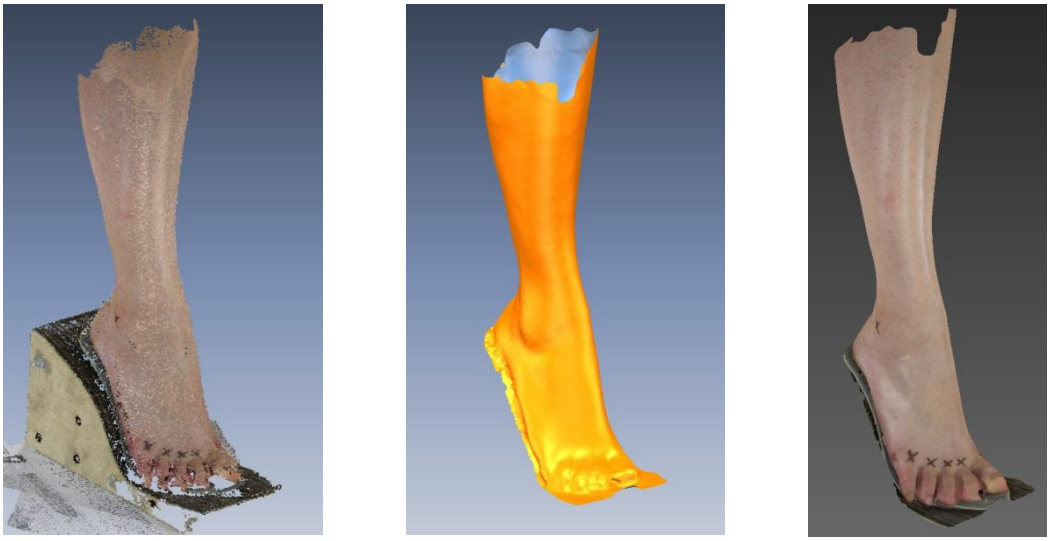

Figure 3 – Five aligned colour point clouds exported from the 3D foot and ankle scanning system (left). Polygonal mesh model created from raw scanned data with Rapidform XOR3 (middle). High definition textural information mapped onto mesh model (right).

2.2 System Validation

To assess the measurement performance of a measurement system, both its repeatability and accuracy has to be examined. According to ISO 5725-1:1994, accuracy is defined as "the closeness of agreement between a test result and the accepted reference value", while precision describes "the closeness of agreement between independent test results obtained under stipulated conditions". [22]

An accurate measurement contains small systematic errors whilst good repeatability indicates small random errors [22,23]. A reliable measurement system should be able to produce both accurate and precise measurements, which are close to and tightly clustered around the reference value.

While accuracy of a measuring system can be examined through comparing the difference between its measurements and the reference value, precision of a measuring system of specific application can be assessed through its measurement repeatability - the quality of measurements that reflects the closeness of the results of measurements of the same quantity performed under the same conditions [23].

Therefore, in this study, three tests were carried out to evaluate the measurement performance of the 3D foot and ankle scanning system: (1) repeatability test, (2) measurement accuracy test, and (3) validation of foot anthropometric measurement extraction – accuracy test for colour information.

In order to eliminate the effects of body sway and movements on the test results, a rigid mannequin was used as the test object to evaluate the performance of the new system. The measurement discrepancies contributed by object deformation could therefore be regarded as negligible [24, 25].

This mannequin has a matte surface with a skin colour which approximates human skin conditions. In addition, its foot features such as the toes and nails are more profound (see Figure 4) and can provide greater levels of details to assess the system's ability.

Figure 4 – Detailed foot features of mannequin used in study.

2.2.1 Repeatability test

A reliable scanning system should always provide the same scanning result under the same scanning conditions, such as the position of the scan object and lighting. An experiment was therefore designed and carried out to assess the repeatability of the 3D foot and ankle scanning system. A total of 12 sets of scans were performed on the mannequin for the repeatability test. The mannequin was first placed in a designated scanning position (P1). Six scans were taken. The mannequin was then rotated about 30 degrees clockwise (P2). Another six scans were taken. The system was switched off and on between each scan.

All of the raw scan data, that is, the point clouds, were processed by using Rapidform XOR3 under the same computation parameters to produce mesh models. These mesh models were then superimposed and the mesh deviations of three randomly selected pairs (1) among the scans acquired in P1; (2) among the scans acquired in P2; and five randomly selected pairs (3) between scans obtained in P1 and P2, were evaluated. The accumulated areas (in percentage of the total mesh area) over the mesh deviations were computed for each pair at 0.1 mm increments [26].

2.2.2 Accuracy test – benchmarking with high quality optical scanner

In this test, the 3D foot and ankle scanning system was compared with a market-available optical scanner, the Comet® Vario Zoom 400 Scanner (Steinbichler Optotechnik GmbH). The scanner provides sequentially projected binary fringes with white light as the projection pattern. Its data accuracy is up to ±0.07 mm, which is much better than the sub-millimeter accuracy claimed by most modern foot scanning systems [20].

A total of 39 partial scans were performed by the Comet® Vario Zoom 400 scanner (see Figure 5). These partial scans were merged to create a single mesh model with Rapidform XOR3. Figure 6 shows the final mesh output. This mesh model was used as a reference model and was compared against the six mesh models previously created with the 3D foot and ankle scanning system at P1 in the repeatability test. The accumulated areas (in percentage of the total mesh area) over the mesh deviations were computed for each pair at 0.1 mm increments. The mesh deviations could be regarded as the measurement errors of the tested scanning system.

Figure 5 – Scanning of mannequin with Comet® Vario Zoom 400 scanner (Steinbichlar Optotechnik Gmbh)

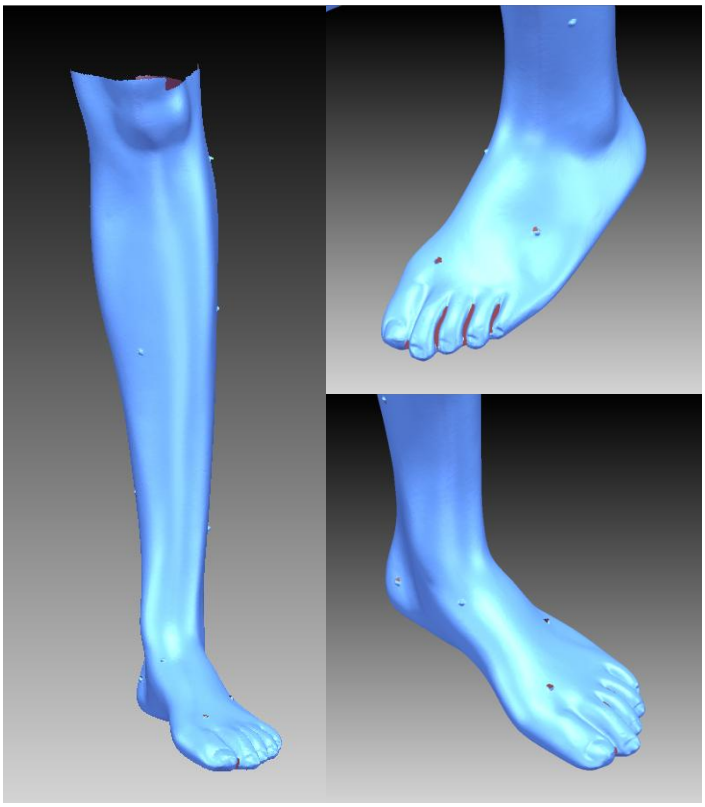

Figure 6- Collection of images that show mesh model created with scans from Comet® Vario Zoom scanner

2.2.3 Validation of foot anthropometric measurement extraction – accuracy test for colour information

The 3D foot and ankle scanning system was designed for scanning the foot with elevation of the heel such that anthropometric measurements could be extracted from the digital scan models. Apart from assessing the spatial accuracy of its resultant models, it is equally important to assess the accuracy of the colour and textural components of the scanned models, which would in turn affect the accuracy of locating any colour landmarks to be used in the foot scanning exercise. Thus, by evaluating the accuracy of the landmark distances extracted from the scans, the textural data accuracy could be validated.

Since the Comet® Vario Zoom 400 Scanner does not record colour in its scans, a digital caliper (measurements are recorded to the nearest 0.01 mm) was used to measure the landmark distances on the reference mannequin.

First, nine landmarks (as shown in figure 7) were identified on the right foot of the mannequin and marked with an "x" with a red ballpoint pen that has a 0.5 mm line weight. Since some of the bone features were not depicted on the mannequin, these landmarks were only the approximation of the anatomical landmarks of a real human foot. Eight linear distances (please refer to Table 1) between these nine landmarks were then measured on the mannequin with a digital caliper by a single examiner. These dimensions were chosen such that the lengths, widths and heights in different magnitudes could be examined across different parts of the foot. They did not correspond to the foot dimension definitions that were commonly used in foot anthropometry. The same set of linear measurements was extracted from three randomly selected mesh models acquired in P1 by the same examiner with the use of Rapidform XOR3. Three rounds of measurements were carried out and the average value of each distance measurement parameter was evaluated.

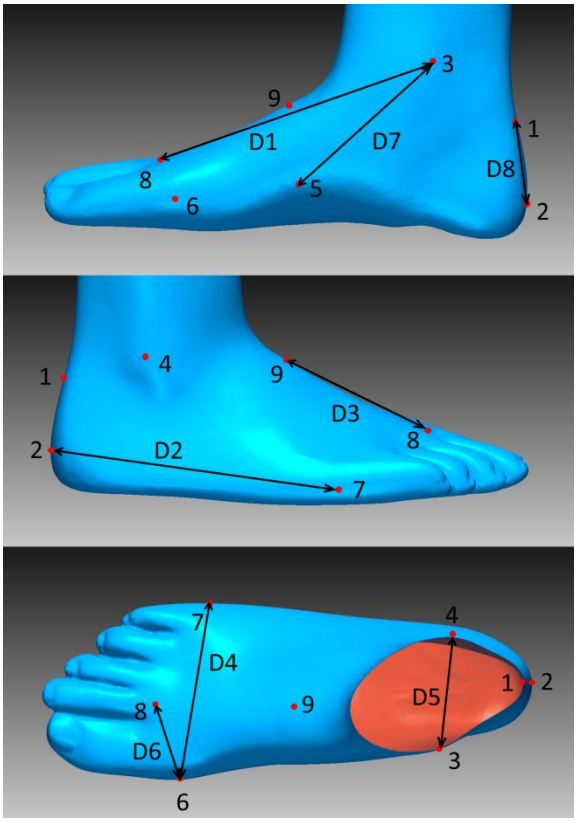

Figure 7 – Medial (top), lateral (middle) and dorsal views that show landmark locations marked on mannequin.

Table 1 – Linear measurement parameters extracted from the reference mannequin.

Linear measurement (Dominant direction vector)	**From Landmark**		**To Landmark**	
D1 (Length)	3	most medially protruding point of the medial malleolus	8	top of the distal inter-phalangeal joint of the second toe
D2 (Length)	2	pternion (posterior point of the heel)	7	the most laterally prominent point on the fifth metatarsal head
D3 (Length)	8	top of the distal inter-phalangeal joint of the second toe	9	Second tarsometatarsal joint
D4 (Width)	6	the most medially prominent point on the first metatarsal head	7	the most laterally prominent point on the fifth metatarsal head
D5 (Width)	3	most medially protruding point of the medial malleolus	4	most laterally protruding point of the lateral malleolus
D6 (Width)	6	the most medially prominent point on the first metatarsal head	8	top of the distal inter-phalangeal joint of the second toe
D7 (Height)	1	junction between achilles tendon and calcaneus (heel bone)	2	pternion
D8 (Height)	5	navicular	3	most medially protruding point of the medial malleolus

Statistical analysis was carried out on all of the measurement parameters. Independent sample t-testing was carried out to evaluate the statistical significance of the differences between the two different measurement methods. Significance was established at $p = 0.05$.

2.3 Foot measurements of elevated heels

2.3.1 Foot scanning on human subjects

In order to study the foot anthropometry with elevated heels, a total of 45 subjects (21 – 35 years old, 160.3 ± 5.7 cm; 53.6 ± 5.8 kg) were recruited to undergo 3D foot scanning with the 3D foot and ankle scanning system. All of them did not have visible foot deformities and were free from foot injuries in the past three years. The study was approved by the Human Subjects Ethics Sub-committee of the Hong Kong Polytechnic University. All of the participants signed written informed consent prior to the implementation of the experiments.

Prior to scanning, the height and weight of the subjects were recorded by using a weight scale and a height rod respectively. Ten anatomical landmarks [27] were marked on their right foot with an eyebrow pencil. A total of three scans (with elevation of 0 cm, 5 cm and 10 cm of the heels) were performed for each subject. During the scanning, the subjects were required to stand still on a flat wooden pile (elevation of 0 cm heel) or a pair of foot supports (with elevated heels) in a balanced

position, with each foot supporting approximately half of the body load. To help the subjects to locate their foot onto the designated position, the foot supports were positioned by the operator. The subjects will then be asked to place their feet onto the supports. To ensure subjects' feet were put correctly onto the foot supports, they were asked to adjust and position their metatarsal-phalangeal joints (MPJ) and arch according to the profile of the foot supports in each scan. The separation of the feet was kept approximately constant cross different heel elevation conditions through measuring their heel-to-heel distance with a ruler.

The three conditions of the heels were scanned in random order. Figure 8 shows a subject who is standing on a pair of foot supports with an elevated heel of 10 cm. To minimise the scanning errors introduced by body swaying due to fatigue, all of the scanning was completed within two minutes and a two-minute break was allowed between the scans.

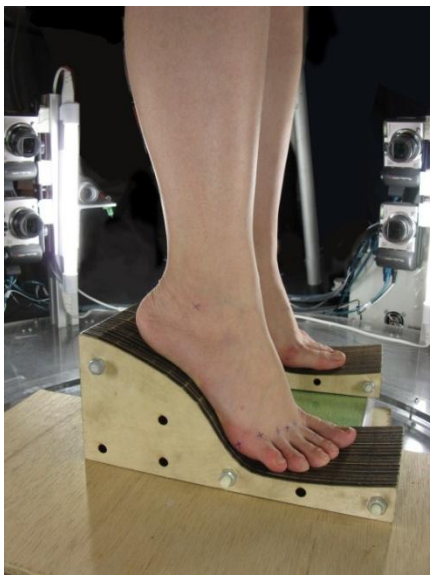

Figure 8 – Subject standing on pair of foot supports with an elevated heel of 10 cm

To simulate an elevated heel of 5 cm and 10 cm, three pairs of foot supports were produced. The profiles of these foot supports are fabricated based on the shoe profiles provided by a shoe manufacturer. The foot supports are made of wood piles with a thickness of 1 cm. These wood piles were cut into the designated shapes by laser and then stacked and tightly fastened together by means of plastic rods and screws.

All of the scanned data were processed in RapidForm XOR3. The resultant 3D mesh foot models were re-aligned such that (1) the floor is aligned with the x-y plane and (2) the foot axis, which is defined by the line that joins the pternion and second metatarsal-phalangeal joint (MPJ), lies along the y-axis when projected onto the x-y plane.

2.3.2 Foot anthropometric measurement extraction and evaluation

In order to study the shape characteristics of the forefoot area, 18 measurement parameters including two toe angles, two toe lengths, three widths across the metatarsal head area, five metatarsal-phalangeal joint (MPJ) heights and five distal interphalangeal (DIP) joint heights were extracted from each scan. These measurements were selected based on the measurements of the flattened shoe last patterns around the forefoot area [28]. Definitions of the measurement parameters are provided in Table 2 and illustrated in Figure 9 below.

Since the position of the heel would change significantly in different elevation conditions, it did not serve as a good reference for the foot measurements. Instead of pternion and heel width points, which were widely used as the reference points for foot measurements in previous studies [27, 29-33], the toe angles and length measurements in this study were referenced to the ball axis and the tread point respectively. The ball girth was excluded in this study because it does not provide much detailed information about the shape characteristics of the forefoot. In replacement the width and MPJ height measurements of each toe were evaluated.

Table 2 – Definitions of forefoot measurement parameters

Definition of foot dimensions			
Foot Axis		Vector that runs from the pternion to the second MPJ projected on the x-y plane	
Ball Axis		Vector that joins the most laterally prominent point of the first and the fifth MPJs on the x-y plane	
Tread Point		Intersecting point between the foot axis and ball axis	
Angle	A1	Flex Angle	Angle between the foot axis and ball axis measured on the horizontal plane
	A2	Hallux Angle	Angle between the orthogonal ball line and the line that passes through the medial edge of the ball width to the contact point on the hallux side measured on the horizontal plane
	A3	Small Toe Angle	Angle between the orthogonal ball line and the line that passes through the lateral edge of the ball width to the contact point on the side of the small toe measured on the horizontal plane
Length	L2	Hallux Length	Distance from the tread point to the tip of the hallux along foot axis
	L3	2^{nd} Toe Length	Distance from the tread point to tip of the hallux along foot axis
Width	W1	Orthogonal Ball Width	Horizontal distance measured between the most laterally prominent point of the first and the fifth MPJs
	W2	Medial Ball Width	Distance between the tread point and the most medially prominent point of the fifth MPJ along the x-axis
	W3	Lateral Ball Width	Distance between the tread point and the most laterally prominent point of the first MPJ along x-axis
Height	H1 – H5	MPJ Height	Distance measured from the surface of the foot platform to the top of the MPJ of each toe, along the normal of the surface of the foot platform.

	H6 – H10	Height at the DIP Joint	Distance measured from the surface of the foot platform to the top of the distal interphalangeal joint of each toe, along the normal of the surface of the foot platform.

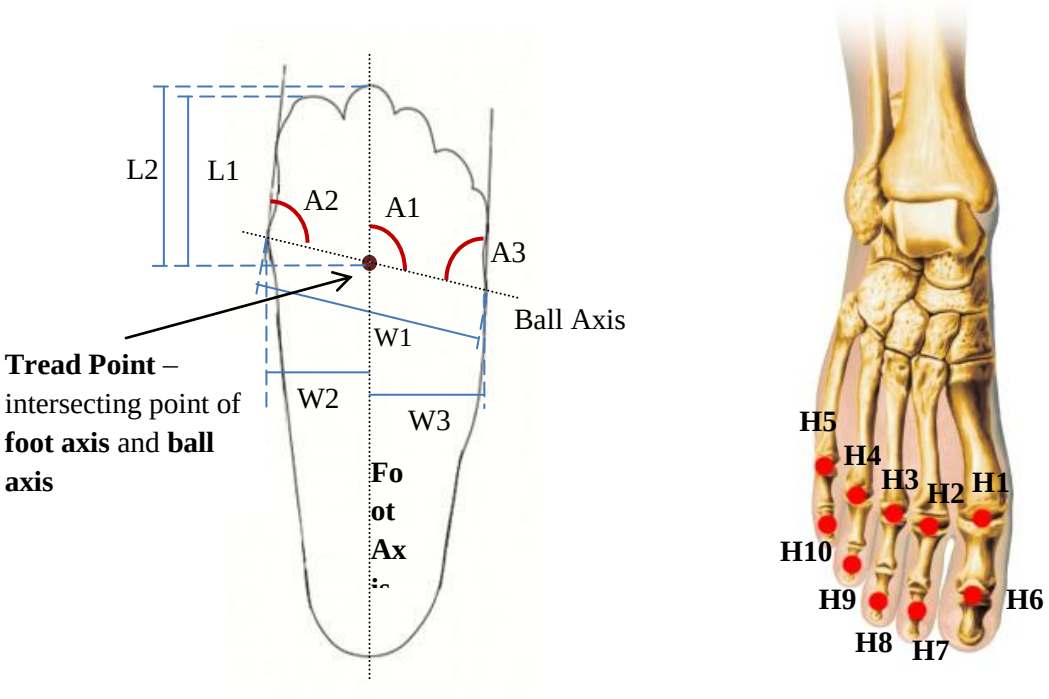

Figure 9 – Dorsal view of measurement parameters: L1-3, A1-3 (left). Dorsal view of locations where H1 to H10 are measured (right).

Statistical analysis was carried out for all 18 measurement parameters with IBM SPSS Statistics 21 software. Repeated measures of analysis of variance (RANOVA) was carried out to evaluate the statistical significance of the differences in the foot measurements measured for the three different heel-heights. Bonferroni post-hoc testing was also carried out to compare the means of all possible pairs of variables measured under the three different heel-heights. Significance was established at $p = 0.05$.

3. Results and Discussion

3.1 Repeatability of 3D foot scanning on mannequin

To evaluate the repeatability of the 3D foot and ankle scanning system, the mesh deviations of three randomly selected pairs (1) among the scans acquired in P1; (2) scans acquired in P2; and five randomly selected pairs (3) between scans in P1 and P2 were evaluated.

For scans acquired in P1, 99.06% of the areas of overlap between the meshes have a deviation less than ± 0.5 mm, and 99.9% within ± 1 mm. Similar results were obtained in P2, where 99.34% of the areas of overlap between the meshes have deviations less than ± 0.5 mm, and 99.98% within ± 1 mm.

Repeatability of the scans that are randomly selected pairs in P1 and P2 is similar (99% within ± 0.5 mm), thus indicating that the repeatability by this system is high when the scans are performed under the same conditions, such as the scan module settings and configurations, positioning of the scan object, and lighting. The system repeatability is comparable to that of a handheld scanner, Artec MHT (Artec Group, USA), which attained a repeatability of 0.6 mm as evaluated by Psikuta et al. [26].

In comparing the scans acquired in P1 with those in P2, the repeatability is reduced. Deviations are less than ± 0.5 mm and ± 1 mm for 93.53% and 99.64% of the accumulated mesh area respectively. The reduced repeatability of the scans that are randomly selected pairs in P1 and P2 indicates that the orientation of the scan modules could affect the coverage and accuracy of the scans, and P1 has a better scanning orientation. This observation also shows that the current positions and orientations of the scan modules have positive effects on the accuracy of the system. Subjects should therefore position themselves on the position and orientation in P1.

3.2 Accuracy of 3D foot scanning on mannequin

In benchmarking the scanning results of the new scanning system against that of the Comet® Vario Zoom scanner for accuracy assessment, it was found that 99.07% of the areas of overlap between the meshes have a deviation less than ± 0.8 mm and 99.59% within ± 1 mm. The accuracy of the system is therefore about ±0.8 mm for over 99% of the areas of overlap between the meshes. This value is well within the measurement tolerance for the designated applications in foot measurement. The smallest measurement unit used in most conventional measuring equipment in anthropometry, such as rulers and tapes, is at the millimeter level. The results of the comparisons in Sections 3.1 and 3.2 are graphically presented in Figure 10.

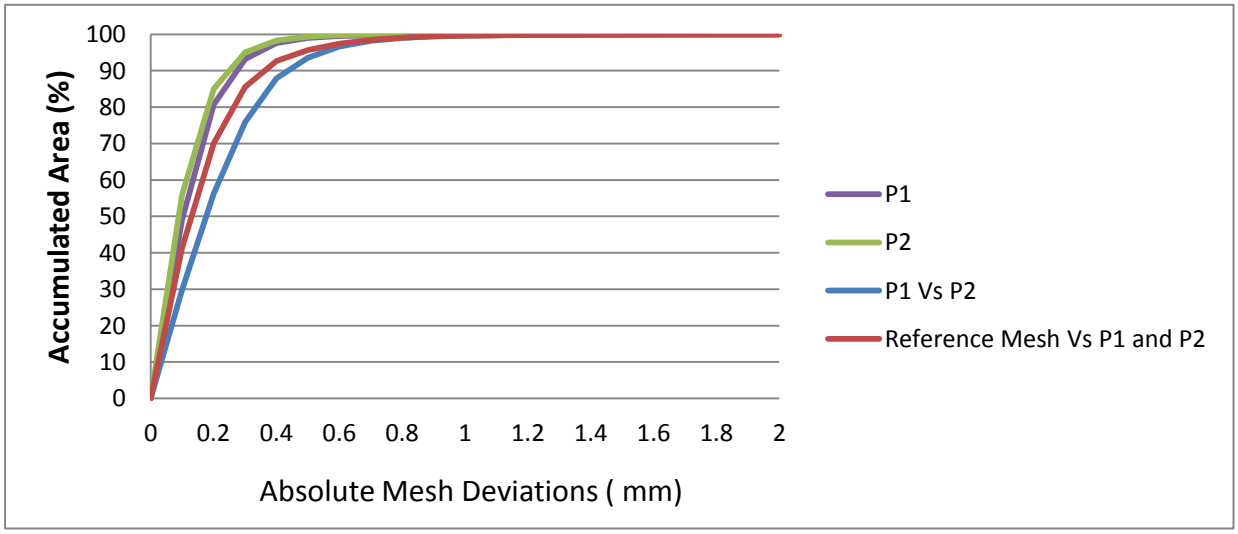

Figure 10 – Graphical presentation of repeatability of scans in (1) P1, (2) P2, (3) randomly selected pairs in P1 and P2, and (4) between reference mesh captured by Comet Vario Zoom scanner and scans in P1

3.3 Comparison with manual foot measurements

Eight linear measurements obtained from the digital caliper and the 3D foot and ankle scanning system were compared with independent sample t-tests. The significance was established at $p = 0.05$. Table 3 summarised the results.

Table 3 – Results of independent sample t-tests that compare and evaluate the mean differences of the two methods. Significance established at $p = 0.05$.

Measurement variable	Digital Caliper		3D foot and ankle scanning system		Mean Diff.	Sig. (2-tailed)
	Mean (mm)	SD	Mean (mm)	SD		
D1 (L)	127.266	.080	127.268	.070	-.002	.971
D2 (L)	**149.354**	**.050**	**149.530**	**.145**	**-.176**	**.050**
D3 (L)	56.272	.046	56.382	.122	-.110	.117
D4 (W)	**90.410**	**.043**	**90.004**	**.312**	**.406**	**.022**
D5 (W)	**55.282**	**.047**	**55.041**	**.214**	**.241**	**.022**
D6 (W)	**39.854**	**.017**	**39.462**	**.104**	**.392**	**.000**
D7 (H)	27.314	.041	27.328	.150	-.014	.848
D8 (H)	63.876	.028	63.79	.205	.086	.403

As shown in Table 3, no significant differences were found between the mean values of the two methods for length and height measurements, except at D2 (mean difference = -0.18 mm). All of the width measurements, D4 (90.00 ± 0.31 mm), D5 (55.04 ± 0.21 mm), D6 (39.46 ± 0.10 mm), which were taken from the 3D models, are less than those measured with the digital caliper, by 0.41 mm, 0.24 mm and 0.39 mm respectively ($p < 0.05$). Moreover, the standard deviations with 3D scanning are generally greater than those with the use of the digital caliper.

The greater standard deviations are because of the mesh model resolution and the measurement extraction method used in the modeling software. In RapidForm XOR3, linear measurements can only be taken between mesh vertices, but not in any other part of the polygonal faces. The extraction accuracy, therefore, is dependent on the mesh resolution. Scanning is a sampling process. The mesh models are digital representations that approximate real objects. Errors are highly possible over the whole digitization process. The mesh resolution of the models is about 0.5 mm while the precision of the digital caliper is 0.01 mm. The standard deviations of the measurements of the 3D foot and ankle scanning system are therefore greater than those of the digital caliper.

The reduced width measurements resulting from the mesh modeling might be related to the smoothing during the mesh building process. Smoothing is usually performed when a mesh is built from a point cloud and during mesh optimization in which the mesh vertices are redistributed to obtain better polygon regularities. Although the mean differences are statistically significant, the discrepancies are

relatively small (<0.5 mm) compared to the new system's accuracy ±0.8 mm (please refer to section 3.2), and are well within acceptable error thresholds for clinical anthropometric data [25, 34].

The test showed that the red landmarks could be easily identified and accurately located on the mesh models, thus indicating that the colour and texture are mapped onto the mesh model with good accuracy and resolution. The texture mapping algorithms adopted by the system are therefore qualified for applications in foot anthropometric measurements.

3.4 Foot measurements of elevated heels

Three angle measurements and fifteen linear foot measurements that encompass all three dimensions were extracted and statistically analysed. Table 4 is a summary of the results from the RANOVA and the Bonferroni post-hoc tests.

Table 4 - Mean, standard deviations, significance of mean differences (RANOVA results) and pairwise significance (Bonferroni post-hoc test results) of each foot measurement parameter for three different heel heights

Measurement Parameter		0 cm	5 cm	10 cm	Sig. of mean difference	
		Mean (S.D.)	Mean (S.D.)	Mean (S.D.)	F	p
Hallux Length	L1	72.301 (±4.51)*¤	73.698 (±4.37)*§	70.788 (±4.54)¤§	25.265	**.000**
Second Toe Length	L2	66.753 (±5.10)*	68.473 (±5.18)*¤	65.492 (±5.32) ¤	16.032	**.000**
Orthogonal Ball Width	W1	90.475 (±5.05)*	90.277 (±5.63)¤	89.046 (±5.10)*¤	12.288	**.000**
Medial Ball Width	W2	38.162 (±2.45)	38.482 (±2.77)	37.861 (±2.41)	2.907	.075
Lateral Ball Width	W3	49.617 (±3.10)*	48.816 (±3.17)*	49.189 (±3.02)	3.538	**.037**
Flex Angle	A1	103.714 (±2.92)*	104.415 (±2.96)¤	101.557 (±3.60)*¤	15.682	**.000**
Hallux Angle	A2	96.729 (±3.69)	97.001 (± 4.85)*	95.191 (±5.86)*	7.577	**.005**
Small Toe Angle	A3	76.686 (±6.00)*¤	78.496 (± 6.44)*§	81.857 (±7.85)¤§	28.196	**.000**
Hallux MPJ Height	H1	26.802 (±1.90)*	26.914 (±1.73)*	26.941 (±1.90)	4.861	**.018**
Second MPJ Height	H2	24.569 (±1.52)*¤	24.154 (±1.44)*	24.079 (±1.54)¤	12.974	**.000**
Third MPJ Height	H3	23.247 (±1.41)*¤	23.662 (±1.58)*	23.737 (±1.56)¤	12.974	**.000**
Fourth MPJ Height	H4	22.418 (±1.59)*¤	23.635 (±1.63)*§	25.101 (±1.94)¤§	86.581	**.000**
Fifth MPJ Height	H5	20.216 (±2.05)*¤	22.570 (±2.16)*§	25.450 (±2.18)¤§	112.706	**.000**
Hallux DIP Joint Height	H6	18.667 (±1.22)*	18.039 (±1.31)	17.888 (±1.16)*	4.469	**.017**
Second DIP Joint Height	H7	13.548 (±1.52)*¤	12.600 (±1.37)*	12.889 (±1.32)¤	12.677	**.000**
Third DIP Joint Height	H8	12.737 (±1.42)	12.453 (±1.29)	12.511 (±1.04)	.986	.381
Fourth DIP Joint Height	H9	12.256 (±1.33)	12.008 (±1.19)	12.114 (±1.27)	.482	.580
Fifth DIP Joint Height	H10	12.793 (±1.57)	12.595 (±1.43)	12.699 (±1.26)	.176	.839

All linear measurements are measured in mm, and angle measurements in degrees.
Significance = $p < 0.05$.
Mean difference pairs with statistical significance: *, ¤ and §.

Toe lengths: Two toe lengths were extracted in the testing: the hallux (first toe; L1) and the second toe (L2) lengths. For both parameters, the longest toe lengths were observed on heels elevated less than 5 cm, with 73.7 mm for L1 and 68.5 mm for L2. The shortest toe lengths were found on heels elevated less than 10 cm, with 70.8 mm and 65.5 mm for L1 and L2, respectively. Statistically significant differences ($p = 0.000$) were observed for both L1 and L2. The significantly shorter toe lengths on heels elevated less than 10 cm (approximately 5 mm shorter than those on heels elevated less than 5 cm) might probably indicate a shift of the tread point towards the toe direction. This hypothesis will be further discussed and verified with other foot measurements later in this section.

Ball widths: Three width measurements were taken in the testing, amongst which significant differences were observed in the orthogonal ball width (W1) and lateral ball width (W3). The greatest orthogonal ball width was found on heels elevated less than 0 cm (90.475 ± 5.05 mm), followed by heels elevated less than 5 cm (90.277 ± 5.63 mm), and finally, heels elevated less than 10 cm (89.046 ± 5.10 mm). Although the mean differences were found to be statistically significant in RANOVA ($p=0.000$), the differences are small (greatest difference is 1.429 mm) when compared with the standard deviation (around ±5 mm). The level of mean differences could be considered as negligible.

Flex angles: The flex angle (A1) was found to be the greatest on an elevated heel of 5 cm (104.415° ± 2.96°), followed by an elevated heel of 0 cm (103.714° ± 2.92°) and finally an elevated heel of 10 cm (101.557° ± 3.60°). The flex angle value for the an elevated heel of 10 cm was found to be significantly different from that for the lower heels of 0 and 5 cm, thus indicating that either (1) the pternion medially shifts relative to the forefoot as the heel is lifted, thus resulting in rotation of the foot axis in the clockwise direction or (2) the ball axis rotates in an anti-clockwise direction on the horizontal plane as the heel is increased, or (3) both situations happen at the same time. More supplementary information will be provided to support (2) when examining the toe angles and MPJ heights later.

Toe angles: Two angle measurements were extracted to explain for the toe spread. For the hallux angle (A2), a significant difference was found between an elevated heel of 5 cm (97.001° ± 4.85°) and 10 cm (95.191° ± 5.86°), with the largest and smallest values among the three heel heights, whilst the small toe angle (A3) increases with heel elevation. The mean small toe angles increased from 76.686° on an elevated heel of 0 cm to 78.496° on an elevated heel of 5 cm, and the highest angle is 81.857° on an elevated heel of 10 cm.

It is interesting to observe that with an elevated heel of 10 cm, the hallux angle is the lowest but the small toe angle is the greatest, and the increase in the angle of the small toe (5.171° compared with an elevated heel of 0 cm) is greater than the reduction in the angle of the hallux (-1.538° compared with

an elevated heel of 0 cm). This phenomenon possibly indicates that (1) the ball axis rotates in an anti-clockwise direction, and (2) the fifth toe laterally shifts with increased heel elevation.

MPJ heights: Although statistically significant differences were observed in all of the MPJ heights for all three tested heel heights, the mean differences for the hallux, and second and third toes are very small, which are less than 0.5 mm. More obvious increasing trends were observed for the fourth and small toes as the heel height was increased. The MPJ heights of the fourth toe increased from 22.418 ± 1.59 mm on an elevated heel of 0 cm, to 23.635 ± 1.63 mm on an elevated heel of 5 cm, and the greatest on an elevated heel of 10 cm (25.101 ± 1.94 mm). The same trend of increase was observed for the MPJ heights of the small toe. The MPJ height values for an elevated heel of 0, 5 and 10 cm are 20.216 ± 2.05 mm, 22.570 ± 2.16 mm and 25.450 ± 2.18 mm respectively. The increase in the MPJ heights in the fourth and smallest toes indicates that the lateral forefoot is lifted as heel elevation is increased, thus resulting in a smaller contact area between the plantar and the sole, and also shifting the body load to the metatarsal heads of the remaining three toes. This explanation accords with previous studies in which plantar pressures were found to be the highest on the hallux and medial forefoot [3-5] with increased heel height.

Lifting of the lateral forefoot also indicates a shift in the ball axis. By combining this observation with the aforementioned observations in the angle measurements (A1 to A3), it can be concluded that the ball axis rotates in an anti-clockwise direction as the heel is elevated. This also explains why the toe lengths are shorter when the heels are elevated to 10 cm. As the ball axis rotates in the anti-clockwise direction, the tread point, based on which the toe lengths are measured, moves towards the direction of the toes. Therefore, shorter toe lengths are observed.

DIP joint heights: Significant differences were identified only in the DIP joint heights of the hallux and second toes. The DIP joint height values on an elevated heel of 0 cm for both toes were found to be greater and significantly different as opposed to an elevated heel of 5 and 10 cm. This indicates that the hallux and the second toes are pressed downward as the heel is elevated. This observation, however, only describes a "general" situation. When examining the digital models, it was observed that the shape of the toes changes quite differently as the heel is elevated. Instead, a number of hammer and mallet toes were found on an elevated heel of 10 cm (Figures 11a and 11b). Of the 50 subjects, mallet toes were observed in four, while hammer toes were found in another eight of the subjects. Such deformities were mainly observed in the second (12 out of 12 occurrences), third (6 out of 12) and fourth (3 out of 12) toes. The occurrence of mallet toes explains the comparatively larger deviations of the DIP joint height measurements of the second toe compared to the other toes.

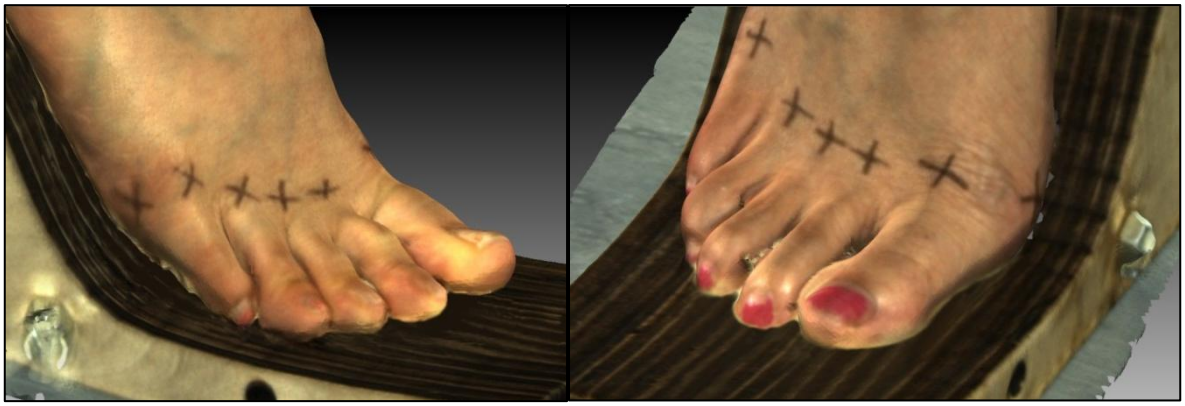

Figures 11a (left) – Hammer toes observed in the 2nd and 3rd toes of one subject. Figure 11b (right) – Mallet toes observed in 2nd, 3rd and 4th toes of another subject.

It is interesting to note that the standard deviations of the linear foot measurements are comparatively greater in consideration of the level of mean differences detected. This is not surprising as these measurements are not normalised to the foot length of the subjects. Measurements of larger magnitudes would therefore result in larger standard deviations in the ratio for a normally distributed dataset.

Generally, the results of this study demonstrate that the forefoot shape changes with different heel elevations as statistically significant mean differences are identified in many of the foot measurements. With increased heel elevation, the toe spread is greater with the fifth toe moving to the lateral side of the foot, and the MPJ height of the fourth and fifth toes is increased.

Moreover, the toes might "deform" with an overly high heel. Toe deformations are observed on the second toe on an elevated heel of 10 cm in almost one quarter of the subjects in this study. The forefoot experiences greater load as the heel elevation is increased, and the shape and placement of the toes change from their natural foot flat position to cope with the extra load exerted.

The findings suggest that slight compensations might be required in the toe box design for better shoe fit and comfort with shoes of different heel heights. The design of a shoe last might involve over 30 foot measurements [35, 36]; however, these measurements should be taken in barefoot in the natural foot flat position. Changes in the forefoot shape characteristics such as a wider small toe angle as the heel height is increased are not considered when making the shoe last for HHSs.

The toe box design is important in footwear as most of the design work takes place at the toe region [28]. On the one hand, the toe box should have enough allowance to account for the movement of the foot inside the shoe and any swelling after long hours of wear. On the other hand, the toe box should not be overly spacious because it needs to grip the foot and restrict the foot into a proper position. As the forefoot bears greater loads and swelling might be increased when wearing HHSs, the toe box

design is particularly critical in HHSs. Compensation might be required in the toe box design with increases in heel height.

Limitations of the study

Reliability and accuracy are evaluated based on mesh models produced in Rapidform XOR3. The results might vary if another post-processing software is used.

Shifting and rotation of the ball axis were observed with increased elevation of the heels. Thus, the ball axis, together with its child component, the tread point, does not appear to be the best choice to align the foot models. A more reliable foot alignment method, which is developed based on anthropometric features with minimal changes over different heel elevations, would be required to bring the foot models of different heel elevations to the same coordinated space for better comparison and description of their shape changes.

Moreover, the foot plantar is not scanned in this study. If accurate scanning of the foot plantar is carried out, more information such as the contact area could be obtained. This would help researchers to understand how the toes "deform" with different heel elevations.

4. Conclusion

The newly developed 3D foot and ankle scanning system in this study has demonstrated repeatability and accuracy for applications that extract anthropometric foot measurements. The system even has the capability to detect minor changes in the forefoot dimensions with variations in the heel height in the foot scanning experiments. The availability of colour and texture information allows for easy landmarking (use of 2D markers instead of 3D markers) during foot scanning. Visible skin conditions of the foot, such as redness, blisters, corns and calluses, could also be identified in the colour foot scans. The short capture time (within 1 second) is also an advantage of the system when human subjects are involved in the scanning process. Measurement errors introduced by unintentional body swaying are minimised since scanning is completed in a very short time span.

To the best of the knowledge of the authors, the current study is the first to focus on forefoot measurements with different heel heights. The shape characteristics of the forefoot, as illustrated by the various length, width and height measurements, are shown to change with different heel elevations. The most obvious observation is a wider toe spread in the horizontal plane, thus indicating that slight compensations might be required in the toe box design when fabricating shoes of different heel heights, especially in the MPJ regions of the fourth and fifth toes and the DIP region of the hallux and second toes.

The deliverable of this study will contribute to the field of footwear design and provide a reliable means for anthropometric measurements. With a fast scanning speed and ease of module reconfigurations, the new scanning system will greatly contribute to the evaluation of:

- fit of HHSs by comparing foot scans with different shoe last models,
- changes in the foot dimensions due to swelling after running or wearing of HHSs for long hours,
- changes in the foot shape at different stages of the stance phase in gait (as a series of 3D measurements can be captured over time by replacing the digital cameras with high-speed cameras), and
- postural studies in scoliosis or breast research where human subjects are to be scanned at specific body bending angles.

Acknowledgement

The authors would like to thank the Departmental Grant of Institute of Textiles and Clothing, The Hong Kong Polytechnic University (grant number PolyU RTLC) for funding this project, and Industrial Centre of the Hong Kong Polytechnic University for providing the scanning modules for the system setup.

References

[1] EDGE Research (2014). *Public Opinion Research on Foot Health and Care*. Retrieved from http://www.apma.org/files/APMA2014TodaysPodiatristSurveyAllFindings.pdf

[2] Snow, R. E., Williams, K. R., & Holmes, G. B. (1992). The effects of wearing high heeled shoes on pedal pressure in women. *Foot & Ankle International*, 13(2), 85-92.

[3] Speksnijder, C. M., vd Munckhof, R. J., Moonen, S. A., & Walenkamp, G. H. (2005). The higher the heel the higher the forefoot-pressure in ten healthy women. *The foot*, 15(1), 17-21.

[4] Lee, K., & Hong, W. (2005). Effects of shoe inserts and heel height on foot pressure, impact force, and perceived comfort during walking. *Applied Ergonomics*, 36, 355-362.

[5] Mandato, M. G., & Nester, E. (1999). The effects of increasing heel height on forefoot peak pressure. *Journal of the American Podiatric Medical Association*, 89(2), 75-80.

[6] Branthwaite H, Chockalingam N, Greenhalgh A. (2013) The effect of shoe toe box shape and volume on forefoot interdigital and plantar pressures in healthy females.(Research)(Report). *Journal of Foot and Ankle Research*. 6:28.

[7] Kouchi, M. (2013). High-Heeled Shoes. In Goonetilleke, R and Ebrary, Inc (Eds). *The Science of Footwear* (pp. 262-277). CRC Press.

[8] Frey, C., Thompson, F., Smith, J., Sanders, M., & Horstman, H. (1993). American Orthopaedic Foot and Ankle Society women's shoe survey. *Foot & Ankle International*, 14(2), 78-81.

[9] Menz, H. B., & Morris, M. E. (2005). Footwear characteristics and foot problems in older people. *Gerontology*, 51(5), 346-351.

[10] De Castro, A. P., Rebelatto, J. R., & Aurichio, T. R. (2010). The relationship between foot pain, anthropometric variables and footwear among older people.*Applied ergonomics*, 41(1), 93-97.

[11] Janisse, D. J. (1992). The art and science of fitting shoes. *Foot & Ankle International*, 13(5), 257-262.

[12] Luximon, A., & Luximon, Y. (2009). Shoe-last design innovation for better shoe fitting. *Computers in Industry*, 60(8), 621-628

[13] Kos, L., & Duhovnik, J. (2002). A system for footwear fitting analysis. In *DS 30: Proceedings of DESIGN 2002, the 7th International Design Conference, Dubrovnik*.

[14] Leng, J., & Du, R. (2006). A CAD approach for designing customized shoe last. *Computer-aided Design and Applications*, 3(1-4), 377-384.

[15] Xiong, S., Zhao, J., Jiang, Z., & Dong, M. (2010). A computer-aided design system for foot-feature-based shoe last customization. *The International Journal of Advanced Manufacturing Technology*, *46*(1-4), 11-19.

[16] Wang, C. S. (2010). An analysis and evaluation of fitness for shoe lasts and human feet. *Computers in Industry*, 61(6), 532-540.

[17] Kouchi, M., & Tsutsumi, E. (2000). 3D foot shape and shoe heel height. *Anthological Science*, 108(4): 331-343.

[18] Au, E. Y. L., & Goonetilleke, R. S. (2007). A qualitative study on the comfort and fit of ladies' dress shoes. *Applied Ergonomics*, 38(6), 687-696.

[19] Tomassoni D., Traini E., Amenta F.(2014). Gender and age related differences in foot morphology. *Maturitas*. 2014;79(4):421–7.

[20] Wan K. W. F., Yick. K.L., Yeung K. L., Yu W., Wong W. N. (2014) *Limitations of Current 3D Foot Scanning Systems for Foot Geometry Evaluation in High-Heeled Postures*, TBIS, Hong Kong, paper ID 100, 6-8 August 2014.

[21] Heikkilä, J., & Silvén, O. (1997, June). A four-step camera calibration procedure with implicit image correction. In *Computer Vision and Pattern Recognition, 1997. Proceedings., 1997 IEEE Computer Society Conference* (pp. 1106-1112). IEEE.

[22] ISO 5725-1:1994(en) Accuracy (trueness and precision) of measurement methods and results — Part 1: General principles and definitions.

[23] Rabinovich, S. (2010). Ch. 1 - General Concepts in the Theory of Measurements. In *Evaluating Measurement Accuracy a Practical Approach (pp. 1-27).* SpringerLink e-books.

[24] Yu, A., Yick, Kl, Ng, Sp, & Yip, J. (2013). 2D and 3D anatomical analyses of hand dimensions for custom-made gloves. *Applied Ergonomics,* 44(3), 381-392.

[25] Weinberg, S., Naidoo, S., Govier, D., Martin, R., Kane, A., & Marazita, M. (2006). Anthropometric precision and accuracy of digital three-dimensional photogrammetry: Comparing the Genex and 3dMD imaging systems with one another and with direct anthropometry. *The Journal of Craniofacial Surgery*, 17(3), 477-83.

[26] Psikuta, A., Frackiewicz-Kaczmarek, J., Mert, E., Bueno, M. A., & Rossi, R. M. (2015). Validation of a novel 3D scanning method for determination of the air gap in clothing. *Measurement*, 67, 61-70.

[27] Witana, C. P., Xiong, S., Zhao, J., & Goonetilleke, R. S. (2006). Foot measurements from three-dimensional scans: A comparison and evaluation of different methods. *International Journal of Industrial Ergonomics*, 36(9), 789-807.

[28] Luximon, A., & Luximon, Y. (2013). Chapter 11, Shoe-last design templates. In Luximon, A.. *Handbook of Footwear Design and Manufacture* (pp. 217-235). Woodhead Publishing Ltd.

[29] Hawes, M. R., Sovak, D. (1994). Quantitative morphology of human foot in a North American population. *Ergonomics, 37(7),* 1213-1226, DOI: 10.1080/00140139408964899

[30] De Mits S., Coorevits P., Clercq D. D., Elewaut D., Woodburn J. and Roosen P. (2011). Reliability and validity of the INFOOT three-dimensional foot digitizer for patients with rheumatoid arthritis. *J. Am. Podiatr*. Med. Assoc. 101, 198-207

[31] Lee Y. C., Lin G. and Wang M. J. (2014). Comparing 3D foot scanning with conventional measurement methods. *Journal of Foot and Ankle Research*.7:44

[32] Lee Y. C., Wang M. J. (2015). Taiwanese adult foot shape classification using 3D scanning data. Ergonomics, 58:3, 513-523, DOI: 10.1080/00140139.2014.974683

[33] Telfer S., Woodburn J. (2010). The use of 3D surface scanning for the measurement and assessment of human foot. *Journal of Foot and Ankle Research.* 3:19

[34] Saghazadeh M., Kitano N., Okura T. (2015) Gender differences of foot characteristics in older Japanese adults using a 3D foot scanner. *Journal of Foot and Ankle Research.* 8:29, DOI 10.1186/s13047-015-0087-4

[35] Hawes, M. R., Sovak, D., Miyashita, M., Kang, S. J., Yoshihuku, Y., & Tanaka, S. (1994). Ethnic differences in forefoot shape and the determination of shoe comfort. *Ergonomics*, 37(1), 187-196.

[36] Chen, G. X. (2005). *The Last Design*, China Light Industry Press, Beijing. (In Chinese)